Some novel three-dimensional Euclidean crystalline networks derived from two-dimensional hyperbolic tilings

S.T. Hyde and S. Ramsden

Applied Mathematics Dept, Research School of Physical Sciences,
Australian National University,
Canberra, 0200, A.C.T.,
AUSTRALIA

(Stephen.hyde@anu.edu.au)

Running title: Novel 3D nets from 2D geometry

PACS Numbers: 87.75.Kd, 89.75.Hc, 82.75.Fq

Abstract:

We demonstrate the usefulness of two-dimensional hyperbolic geometry as a tool to generate three-dimensional Euclidean (E^3) networks. The technique involves projection from tilings of the hyperbolic plane (H^2) onto three-periodic minimal surfaces, embedded in E^3. Given the extraordinary wealth of symmetries commensurate with H^2, we can generate networks in E^3 that are difficult to construct otherwise. In particular, we form four-, five- and seven-connected (E^3) nets containing three- and five-rings, *viz.* (3,7), (5,4) and (5,5) tilings in H^2. These examples are of fundamental interest, as they present "topological symmetries" that are incompatible with the isometries of E^3.

Keywords:

Non-euclidean crystallography; networks; hyperbolic geometry.

Introduction:

The motivation for this work lies in our poor knowledge of networks in three-dimensional Euclidean space (E^3). The nature of E^3 presents obstacles to net formation that are not yet well understood. Those obstacles are in part *geometric*. Thus, for example, a locally preferred packing configuration corresponding to tetrahedrally close-packed arrangements of vertices is unrealizable in E^3, but accessible in 3D elliptic space. In a series of papers, Sadoc, Mosseri and Rivier have argued that many atomic configurations in glasses and alloys (particularly Frank-Kasper phases and their duals) are frustrated attempts to decurve those elliptic configurations, involving networks of disclinations, and thereby mapping the elliptic geometries back to E^3 (ref. [1]). A number of conjectures concerning accessible ring-sizes in four-connected nets have been made by chemists that remain intriguing yet unproven[2]. It is possible that there are, in addition, *topological* obstacles to net formation in E^3, where certain network topologies are unrealizable with *any* geometry in flat 3D space. Despite the corpus of data on networks gathered by solid state chemists, it is fair to state that we remain in a state of profound ignorance of the variety of nets realizable in E^3. Substantial progress in experimental determination of structures to high resolution of atomic and molecular crystals has not been mirrored by corresponding progress in fundamental understanding of *possible* structures in E^3. We have not advanced much beyond empirical construction of nets, despite advances in systematic enumeration of a restricted class of four-connected nets in E^3 (ref. [3]).

It has long been recognized that crystalline networks, particularly those of low topological vertex density (normalized to nets of unit edge length) are decorations of triply periodic minimal surfaces, or topologically identical surfaces [4,5]. Here we formalize somewhat that construction, and focus on examples that are intractable within the confines of conventional Euclidean crystallography. Net(work)s are constructed with pentagonal rings and containing equivalent seven-connected vertices.

This paper offers some examples of a novel technique to construct nets *ab initio*. The technique is almost exclusively confined to 2D geometry, where the third dimension of E^3 is subsumed within a parameter available to non-euclidean geometries, curvature. Rather than working within flat 3D space (E^3), we construct the unwrapped net in 2D hyperbolic space, H^2 and then project H^2 onto E^3, via triply periodic minimal surfaces.

Construction of 3D euclidean nets from the hyperbolic plane:

The approach involves the formation of a net in its universal cover. There is a simple analogy to cylindrical nets, well developed to characterise carbon tubule structures. In that case, the sp^2 graphite net tiles a cylinder. The (surface averaged) Gaussian curvature of a cylinder (or any extended rod-shaped surface) is zero, and the cylinder is Euclidean. Its universal cover is the Euclidean plane (E^2). The graphite net can be realized as a regular tiling of E^2, with identical vertices, all belonging to three hexagonal rings; we denote the net by a modified Schläfli symbol, (6,3). (The *regular* form of (6,3), with

symmetrically identical hexagonal faces, edges and vertices, is denoted {6,3}.) Tubule nets can be generated by projecting the (6,3) net onto the cylinder, formed by gluing parallel lines traced on E^2. The infinite (6,3) pattern in the unbounded Euclidean plane, E^2, is thus an infinite-sheeted cover of the cylindrical tiling. A realisable carbon tubule structure derived from graphite corresponds to the identification of any 1D lattice on the (6,3) net (Figure 1). The lattice vector defines an equatorial loop around the cylinder and the cylinder dimensions relative to the edge length of the (6,3) tiling. The smallest lattice vector commensurate with the graphite net defines an achiral tubule structure, generic examples are related to this one by a screw disclination.

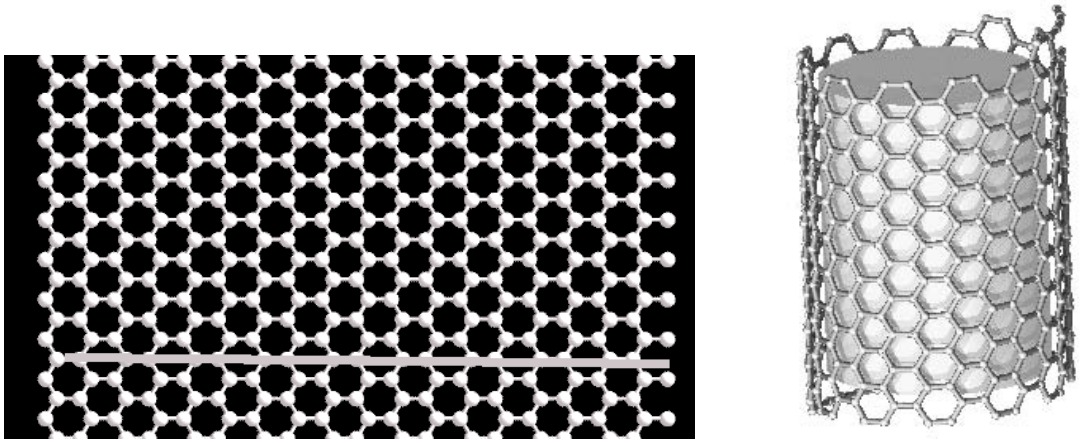

Figure 1: Mapping {6,3} to carbon tubule nets: the graphite network is rolled gluing ends of the equatorial lines (a). The length and orientation of that line determines the tubule radius and chirality resp. (Tubule image courtesy of D. Tomanek.)

Generalisation of this concept allows us to systematically derive examples of a restricted – but large – subset of all crystalline nets in E^3. Those nets tile hyperbolic surfaces, and can be embedded without altering their topology (though likely their geometry: the edge lengths and shapes and vertex positions). The universal cover[6] of hyperbolic surfaces is the hyperbolic plane, H^2, which can be considered as a multiple-copy of the unfolded three-periodic surface, just as the Euclidean plane is the universal cover of the cylinder. Here too, we can generate nets on three-periodic surfaces in E^3, that are crystalline three-periodic nets in E^3, via tilings of H^2. The nets contain surface rings, visible in the H^2 tiling and collar rings, that are the result of the projection (or gluing) from H^2 to the surface.

There is a significant extra complication in this construction, that is not present in the cylindrical examples. That complication arises from the requirement that H^2 be distorted in order to project in onto E^3. In practice, the Gaussian curvature of three-periodic hyperbolic surfaces must vary over the surface, in contrast to the fixed (negative) Gaussian curvature of H^2. The isotropic H^2 space is distorted, and a conformal group structure imposed on H^2 to allow projection onto E^3. The conformal structure can be made exact for the case of three-periodic minimal surfaces, as follows. These surfaces are made up of asymmetric surface patches (*Flächenstücke)* bounded by special curves that are intrinsic mirrors in the surface[7]. Those mirrors emanate from the isolated singular

points on the minimal surface of zero Gaussian curvature, the flat points. Their type and locations are defined by the Gauss map of the surface, used to explicitly parametrise the surface embedding in E^3. Those curves correspond to special directions on the surface (principal or asymptotic directions, with the exception of the gyroid) and are orthogonal at all points except at flat points. The polygons are thus right-angled except at flat points.

We consider here only the simplest three-periodic minimal surfaces, the P and D surfaces and the hexagonal H surface. The Gauss maps of their *Flächenstücke*, resident in the 2D complex plane, C^2 (derived in ref. [7]) are polygons whose edges are circular arcs. The complete surface is generated by reflection in the edges of the polygon. The Gauss map is a conformally faithful representation of the surface geometry in E^3, except at flat points (i), where it is multiplied by the order b_i of the flat point. These polygons, with suitably rescaled vertex angles at vertices corresponding to flat points, thus offer a convenient conformal map for the three-periodic minimal surface geometry in its universal cover (H^2) [8]. The relevant polygons in C^2 are shown in Figures 2. Note that the P and D surfaces are intrinsically identical – only their E^3 embeddings differ – so that their *Flächenstücke* are indistinguishable.

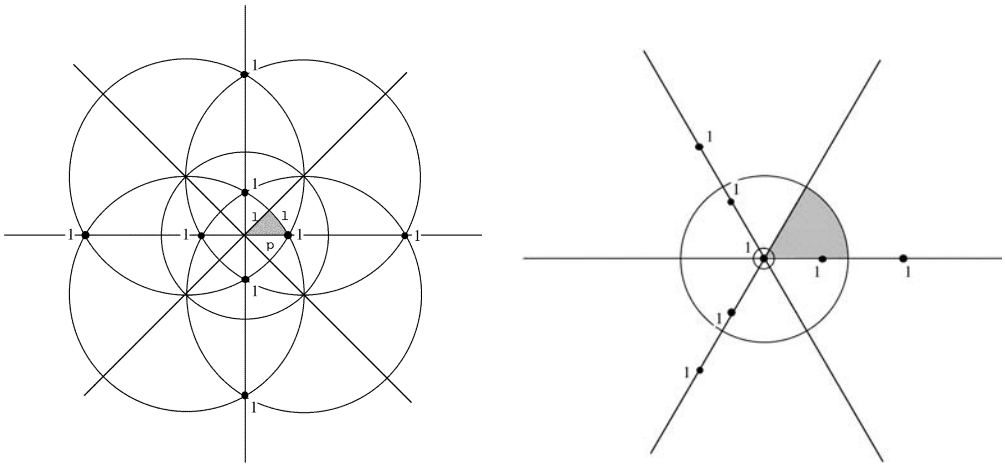

(a) (b)

Figure 2: Complex plane representation of the Gauss map of the P and D three-periodic minimal surfaces (a) and the H surface (b). The maps contain asymmetric tiles (shaded) that generate the complete map by reflection in the tile edges. Flat points on the tile edges are marked by a dot and the numeral 1, denoting that these are first-order flat points. The P/D tile contains three vertices, the H tile four, counting the flat point along an edge. (The open circle at the origin in (b) denotes an extra first order flat point at ∞.)

This construction allows (in principle) an exact conformal map from H^2 to the surface. We are principally concerned with the topological structure of the nets on these surfaces, and their geometry is later relaxed in E^3, so we refrain here from explicit description of that map (that has, in any case, yet to be explicitly determined in most cases).

The conformal maps on H^2 impose a group structure on that space, as the *Flachenstücke* polygons are mirrors. The hyperbolic crystallography of these surfaces is thus a sub-group of the (kaleidoscopic) group defined by these mirrors. The full group defines the relevant group of the universal cover of the surface – unglued into the disc-like hyperbolic plane, and replicated. The three-periodic minimal surface contains relations in addition to the mirrors, defining the gluing pattern needed to stitch the surface up from H^2 (identical to the gluing lines for cylinders from E^2). A detailed account of this procedure for the P and D surfaces can be found [9]Those translations must be respected in any tiling superposed on H^2, to ensure the projected tiling, a net in E^3, is commensurate with the surface and contains the same translational symmetries as those of the underlying surface. (We could relax that constraint, and allow supercells of the surface lattice; here we neglect that possibility.) In order to *reticulate* the three-periodic minimal surface in a commensurate fashion, the starting tiling in H^2 is chosen to be a sub-group of the full kaleidoscopic group of the surface.

The hyperbolic crystallography of these surfaces can be neatly described using the orbifold notation developed by Conway and Thurston[10]. An orbifold contains a single asymmetric unit of the symmetric 2D pattern, suitably compactified. The notation is particularly useful, as it is generic to the three possible 2D non-euclidean geometries: elliptic (e.g. point groups), parabolic or Euclidean (planar groups) and hyperbolic. There are only four possible symmetry elements of these 2D groups: mirrors, glides, rotation centers and translations. Each element has a symbol, and a symbol string defines the group. For our purposes, we need to consider only orbifolds containing rotation centers (denoted by the numeral "*a*", where the rotation center defines an *a*-fold rotational center and mirror lines (contributing a single "*" character per disjoint mirror circuit). Rotation centers lying on intersections of mirror lines subtending angles of $\frac{\pi}{b_1}, \frac{\pi}{b_2}, \ldots$ lead to the "$*b_1\ b_2 \ldots$" character string. For example, the pattern in the complex plane due to the Gauss map of the P or D surfaces (or on the sphere, S^2) contains a single triangular motif, bounded by mirror lines intersecting at $\frac{\pi}{2}, \frac{\pi}{4}, \frac{\pi}{3}$ (Figure 2a). The relevant orbifold symbol string is thus **243*. (Note that cyclic permutation of ordering of rotation center symbols and mirror intersection is allowed.)

The symbol string allows direct reckoning of the *characteristic* of the orbifold, via the equation:

$$\chi = 2 - \sum_i c_i \qquad (1)$$

where c_i values are associated with each character entry in the orbifold symbol (Table 1). This characteristic coincides with the topological Euler-Poincaré characteristic, and scales linearly with the integral Gaussian curvature of the asymmetric domain in the relevant 2D space. Since the spaces are of constant Gaussian curvature, the Gauss-Bonnet theorem implies that the characteristic also scales with the area of the asymmetric domain. If the characteristic is positive, the geometry if elliptic (e.g. spherical 2D groups, the crystallographic point groups); zero implies Euclidean character (usual 2D planar groups); negative characteristics are associated with hyperbolic space.

Symmetry element	Symbol	cost, c_i
Mirror	*	1
Rotation center (cone point)	a	$\frac{a-1}{a}$
Mirror intersection (angle $\frac{\pi}{b}$)	b	$\frac{b-1}{2b}$

Table 1: Character strings and costs associated with 2D symmetry elements of orbifolds. The orbifold characteristic is calculated from these costs (eq. 1). The string nomenclature is applicable to any *2D symmetric pattern, whether it is elliptic, planar or hyperbolic. (Crystallographic point groups are elliptic, 2D planar groups are Euclidean.)*

A second, concise description of the recipe for determining the relevant kaleidoscopic group of the universal cover of the surface is possible with the orbifold concept. Note first that the Gauss map is defined on the unit sphere, S^2, whose universal cover is the elliptic plane. Due to the reflection symmetries of the Gauss map, the elliptic group is a kaleidoscopic group. Symmetry editing, multiplying the order of the mirror points at branch points (i) of the Gauss map by their order, b_i, gives the relevant hyperbolic kaleidoscopic group of the universal cover of the three-periodic minimal surface in H^2. All the surfaces considered here have exclusively first order branch points, so that the mirror points at flat points must be doubled. The correspondence is illustrated in Table 2.

Surface	Gauss map orbifold (S^2, C^2)	Surface orbifold (H^2)
P, D	**243*	**246*
H	**3(1)22*	**6222*

Table 2: Orbifold symmetries for the P, D and H three-periodic minimal surfaces. The surface orbifolds are simple "symmetry edits" of the orbifold of the Gauss map of the surfaces (fig. 2).

The conformal map offers a conformally exact – but non-isometric – mapping from H^2 to the three-periodic minimal surfaces. Conformal equivalence means that all angles are preserved between nets drawn on H^2 and the projected nets drawn on the three-periodic surfaces (in E^3). The lack of isometric equivalence means that edge lengths on the nets differ from H^2 to E^3. But the mapping is sufficient to construct nets in E^3 with specified 2D *topology* from those in H^2. Specific sites on H^2 map to sites on the three-periodic surfaces. An explicit transformation from H^2 to C^2 to E^3 can be established, and will be presented elsewhere. For now, we use the vertices and edges of the kaleidoscopic tiling of the surface orbifold as a coordinate net. We call this net the *surface atlas*. The relevant atlases in H^2 for the P, D and H surfaces are shown in Figure 3.

We use a compact, conformal representation of H^2, known as the Poincaré disc model. This model allows the entire hyperbolic plane to be represented in a unit disc in the euclidean plane, at the expense of much foreshortening of distances while all angles in

H^2 are conserved in the Poincaré disc[11]. The correspondence between points on H^2 and points in E^3 (via Cartesian coordinates on the three-periodic minimal surfaces) follows at once from the identification of the H^2 orbifold with the C^2 orbifold of the Gauss map, since a constructive map from the C^2 coordinates to E^3 cartesian coordinates is afforded by the Weierstrass equations defining the minimal surface geometries[7].

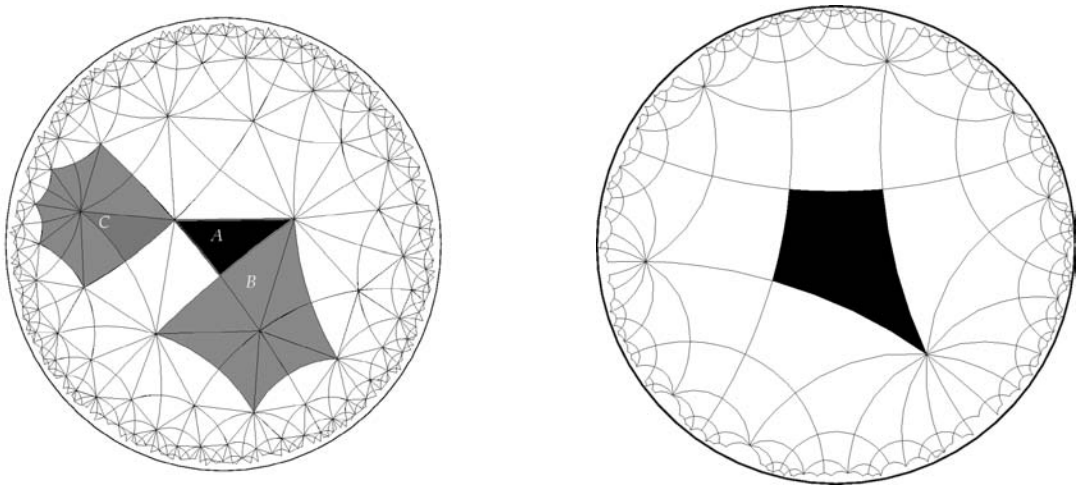

(a) (b)

Figure 3:Surface atlases of the (a) P, D and (b) H surfaces in the Poincaré disc representation of the hyperbolic plane. The atlas is the universal cover of the surface with the surface orbifold symmetry. Single asymmetric units of (a) the *246 *and (b)* *6222 *orbifolds are shaded black. (a) Single asymmetric tile (*A*), a single regular tile of the (*B*) {4,6} and (*C*) dual {6,4} tilings on the P and D surface universal covers.*

The construction leads to three-periodic nets in E^3 with specified 2D ring-size n_2, and edge valency (connectivity) at each vertex, z, whose 2D Schläfli symbol is (n_2,z) in general, and $\{n_2,z\}$ in some cases (with regular n_2-gons) . Collar rings are invisible in the universal cover (H^2); they are not prescribed *a priori*. Just as for graphitic tubule nets of distinct chirality (and screw dislocation strength), multiple nets 3D nets can be constructed sharing the same surface rings, but displaying different collar rings. (A lengthy introduction to our approach has been presented elsewhere[12].)

We illustrate the technique with some examples of network topologies that are difficult to realize within the context of 3D Euclidean space. In particular, we construct examples of (3,7), (5,4) and (5,5) reticulations of the P and D surfaces. The first example is of fundamental interest: it is the simplest hyperbolic analog of the regular close-packing pattern of identical discs in E^2 (i.e. {3,6}) and its seven-fold connectivity cannot be symmetric in E^3. The latter examples, containing pentagonal rings are also of wider interest, due to the geometric frustration of embedding regular pentagonal patterns in E^3.

The crystallography of H^2 is immensely rich compared with 2D (or 3D) Euclidean crystallography. *Any* net (n_2,z) can be embedded in H^2 such that all vertices, edges and rings are symmetrically equivalent (regular), to form {n_2,z}. The examples we consider here are shown in Figure 4. These regular nets {n_2,z} display pure reflection symmetry: they are decorations of the *n_2z2 orbifold.

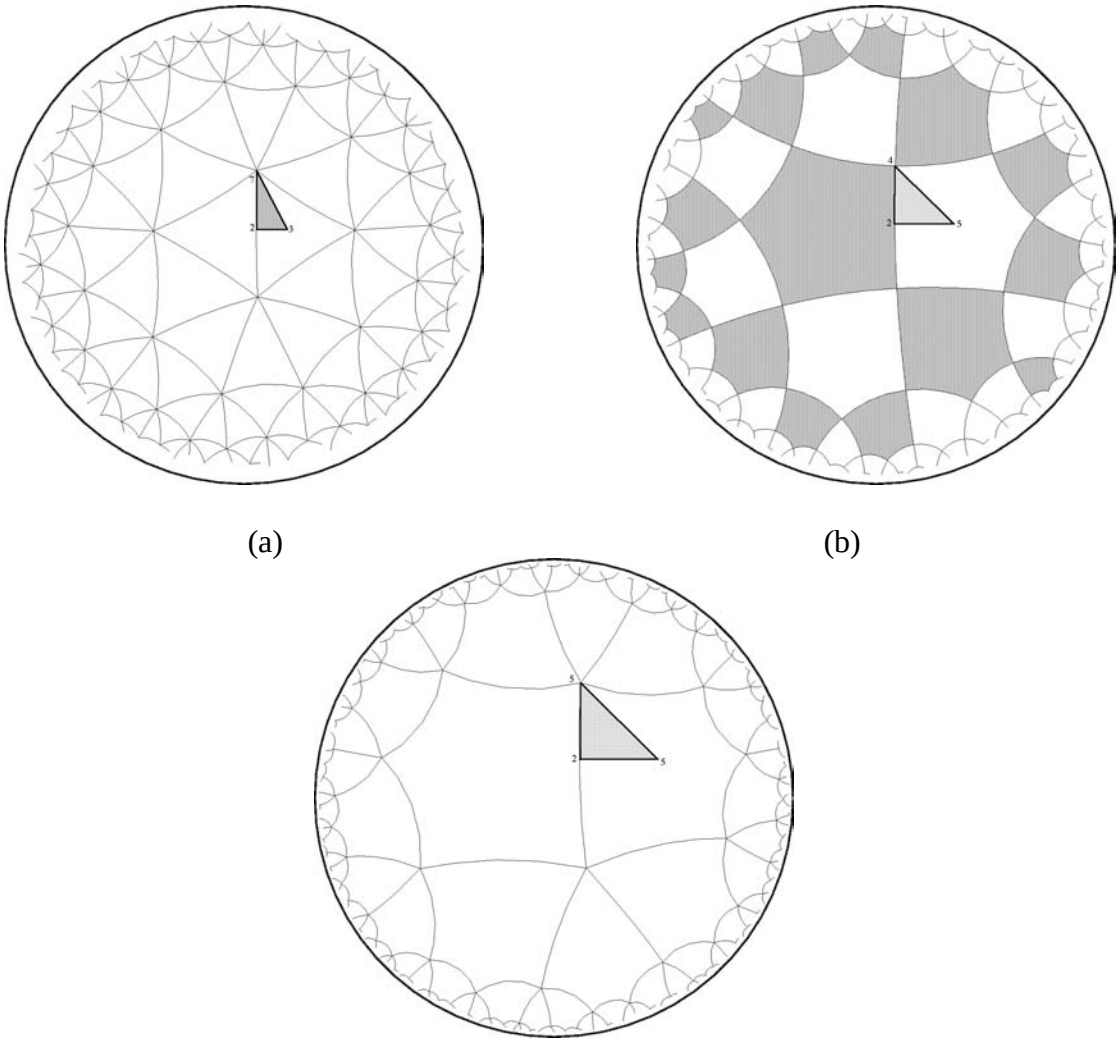

Figure 4: Regular hyperbolic tilings with symmetrically identical vertices, edges and faces; (a) {3,7} (b) {5,4} and (c) {5,5}. Single triangular domains of the relevant kaleidoscopic orbifolds are outlined by dark edges, lying on mirror lines: (a) the *237*, (b)* *245 (ignoring the tile colouring) and (c)* *255 *orbifolds.*

Formation of Euclidean nets:

Projections of hyperbolic tilings onto three-periodic surfaces in E^3 generally requires some symmetry reduction of the regular tiling. A common sub-group (orbifold) to the surface orbifold and the orbifold of the regular tiling must be found. Nevertheless, despite the incommensurability of generic n_2 rings with the structure of E^3 (e.g. pentagons and heptagons), symmetric reticulations are possible. We first construct the (n_2,z) nets in H^2, superposed on the relevant orbifold for the universal cover of the minimal surface. In some cases, that superposition can be done by inspection. The construction can be done more systematically using the following topological constraints. First, locations for vertices and faces of the required (n_2,z) net are chosen. The ring- and vertex density can be derived using Euler's relation, that relates the Euler characteristic, χ, to the number of vertices, V, edges, E and faces, F, in the network:

$$\chi = V - E + F: \tag{2}$$

$$\chi_F = 1 - \frac{n_2}{2} + \frac{n_2}{z} \tag{3}$$

and

$$\chi_V = 1 - \frac{z}{2} + \frac{z}{n_2} \tag{4}$$

where χ_F and χ_V denote the Euler characteristic per face and vertex respectively. The ratios of those characteristics with the characteristic per surface orbifold determines the vertex and face density per surface orbifold.

Consider first the regular {4,6} net, or its dual {6,4}, that comprise a uninodal net in the atlas for the P/D surfaces, and possible superposition of the (5,4) net on that tiling. A solution is evident by inspection in the Poincaré disc model of H^2; that superposition results in a pattern of symmetry **2224*, whose characteristic, from eq. 1 is equal to $\frac{-1}{8}$ (Figure 5). Note that a (6,4) tiling with **2224* symmetry is, in general, distorted, in contrast to {6,4}. The geometry of single **2224* domains is not rigid, as the only constraint on their form is the requirement that vertex angles are equal to $\frac{\pi}{2}$, $\frac{\pi}{2}$, $\frac{\pi}{2}$ and $\frac{\pi}{4}$. We note that hyperbolic *n*-gons with fixed vertex angles have (*n-3*) degrees of flexibility in H^2. Domains of the **2224* tiling of H^2 thus contain a single free parameter, that can be tuned to force the regular {5,4} tiling, superposed on an irregular (6,4) tiling (Figure 5a) and *vice versa* (Figure 5b).

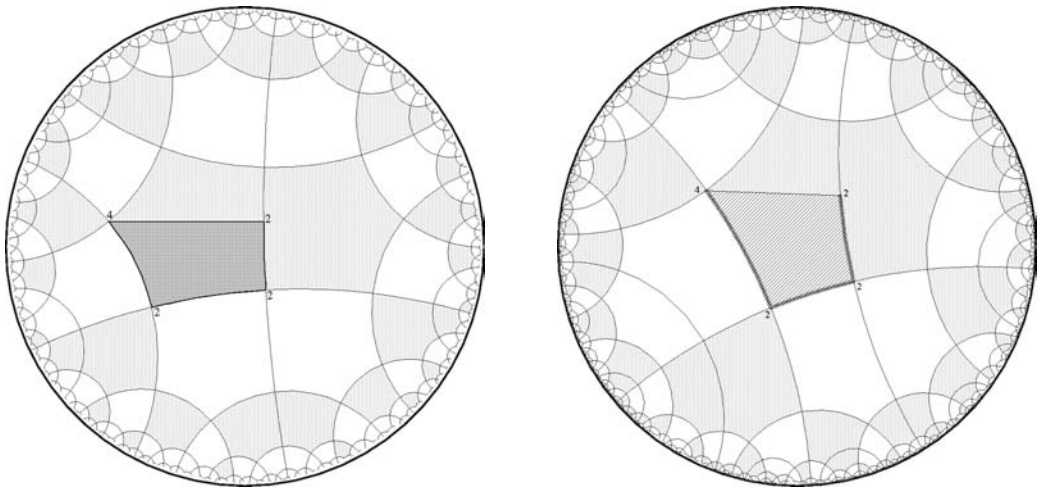

(a) (b)

*Figure5: (a) Superposition of the regular {5,4} tiling on the irregular (6.4) tiling (with (6) rings shaded alternately grey and white for clarity). A single *2224 quadrilateral orbifold domain is highlighted, bounded by mirrors with vertex angles of* $\frac{\pi}{2}, \frac{\pi}{2}, \frac{\pi}{2}$ *and* $\frac{\pi}{4}$. *(b) Superposition of the regular {6,4} tiling (with {6} rings shaded alternately grey and white for clarity) on the (5,4) tiling. A single *2224 orbifold domain is highlighted.*

As required, **2224* is a sub-group of both the P and D surface orbifold, **246* and the orbifold of the regular {5,4} tiling, **245*. Is a more symmetric deformation of {5,4} allowed? That can be established from the characteristics of these orbifolds, *viz.* $\frac{-1}{24}$ and $\frac{-1}{40}$ respectively. The sub-group index follows at once from the ratios of the relevant orbifold characteristics[10]. Common sub-groups to these orbifolds must have indices that scale according to the ratio of the group characteristics: $\frac{40}{24}$. The most symmetric common sub-groups must therefore be of index 3 in **642* and 5 in **542* with characteristic $\frac{-1}{8}$, equal to that of **2224*. We have therefore found a maximally symmetric embedding of {5,4} in the P and D surfaces. It is worth pointing out that the **2224* orbifold is precisely that of the tetragonally distorted family of P and D surfaces, the tP and tD surfaces. That can be inferred from the Gauss maps of the tetragonal family[7] (using the algorithm outlined above.) It follows at once that a more regular geometric embedding of the {5,4} net can be realized by projecting onto the tP and tD surfaces. However, we consider here only the cubic reticulations.

The resulting projections on the (cubic) P and D surfaces are shown in Figure 6.

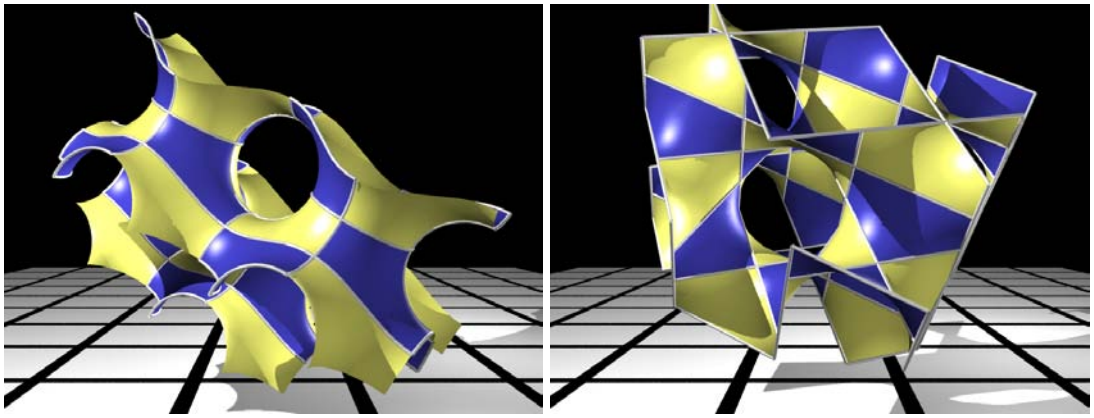

(a) (b)

Figure 6: Projections of the {5,4} onto the (a) P and (b) D minimal surfaces according t the superposition described in Figure 5.

We turn next to the (5,5) tiling. Here too, the superposition of an irregular (6,4) tiling on {5,5} can be determined by inspection (Figure 7a). The arrangement of vertices and edges of the {5,5} net relative to (6,4) provides a topological connection diagram to reconstruct an irregular (5,5) on {6,4}, allowing projection to the P and D surfaces. We use that map to superpose the (irregular) (5,5) tiling on the (regular) {6,4} tiling (Figure 7b). The resulting orbifold symmetry is *22*2*, with characteristic $\frac{-1}{4}$. This orbifold is a sub-group of index 5 relative to the regular {5,5} tiling (**552* orbifold) and index 6 relative to the **642* surface orbifold of the P and D surfaces. Given that the ratio of characteristics of the **552* to **642* orbifolds is $\frac{24}{20}$, the sub-group index ratio of $\frac{6}{5}$ implies, once again, that the pattern is maximally symmetric.

The *22*2* pattern is flexible. Indeed, a specific example of the pattern contains the regular {6,4} tiling (Figure 7c), proving that the superposition of (5,5) on {6,4} is feasible in H^2.

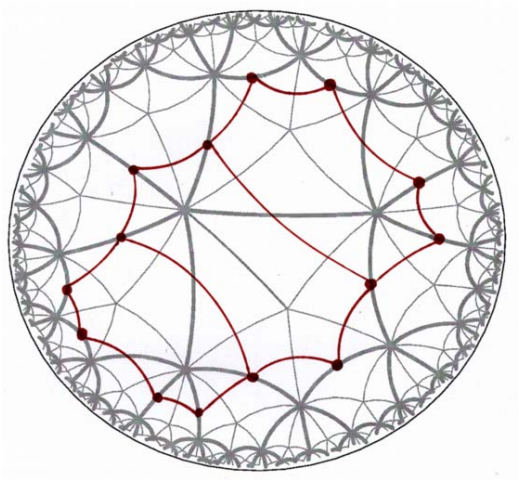

(a)

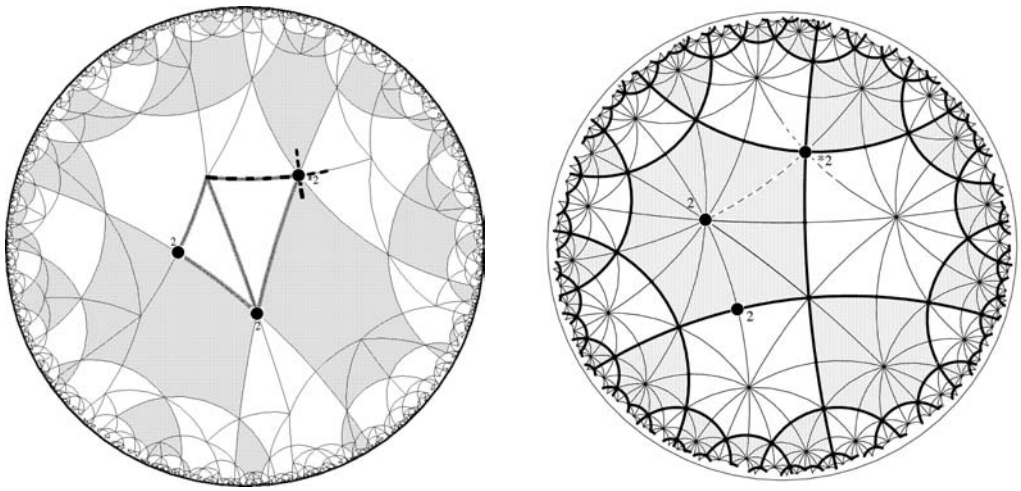

(b) (c)

*Figure 7: (a) Superposition of an irregular (6,4) net on regular {5,5} tiling. The resulting pattern has orbifold symmetry 22*2: thinner arcs lie on mirrors of the *255 pattern characteristic of {5,5}. Edges of {5,5} are thicker arcs; edges of (6,4) are marked by dots. Thicker lines are edges of the {5,5} net.*
*(b) A (5,5) net superposed on a (6,4) net, with 22*2 symmetry. Edges within a single 22*2 domain are thickened, with "2" entries denoting 2-fold rotational symmetry sites, and the "*2" entry the intersecting of a pair of orthogonal mirrors (dotted lines). Alternate (4) tiles are shaded to aid identification of the (6,4) tiling.*
*(c) The regular {6,4} tiling has a subgroup of symmetry 22*2. (b) can therefore be deformed to give (5,5) on {6,4}.*

The projections of this net onto the P and D surfaces are shown in Figure 8. Straightened examples, with all edges geodesic in E^3, are also shown. These nets exhibit a complex and interesting structure. The projection process forms 4-sided collar rings in both cases. The P version, which adopts a tetragonal symmetry in the straightened version, bears a fascinating relation to stacks of intergrown, slightly distorted graphite networks (each with 2-fold rotational symmetry), rotated by $\frac{\pi}{2}$ with respect to each other. These layered intergrowth are interconnected by connections surrounding a 4_1 screw axis, inducing an overall chirality in the net. That chirality is evident from the orbifold decoration (Figure 7a): the bilateral symmetry of the orbifold domain has been broken, and there is an arbitrary choice of two possible diagonal edge orientations. Chirality of the net is visible within the hyperbolic plane pattern, an attractive feature of this technique[12].

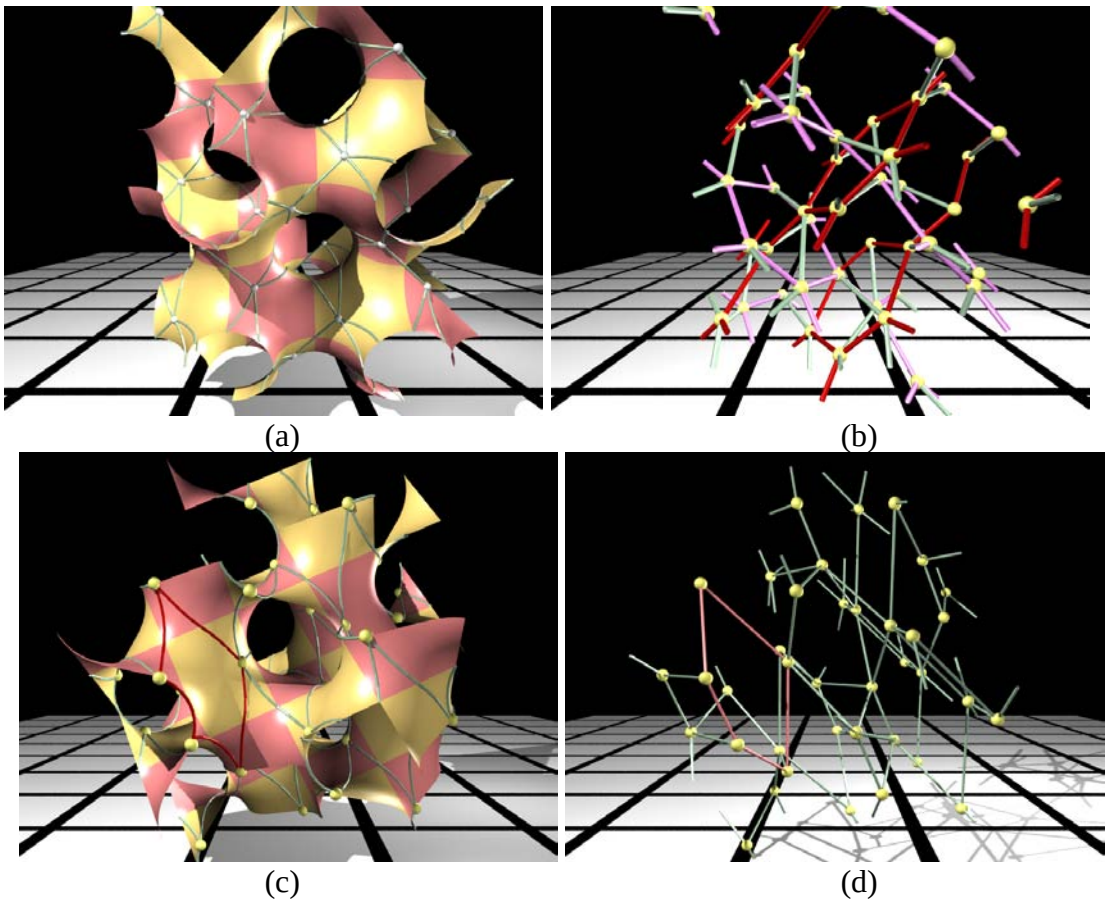

Figure 8: Projections of {5,5} nets onto the (a) P and (c) D surfaces. (b) and (d) have identical vertex positions to those in (a) and (c) respectively, with straightened edges. The presence of intergrown irregular {6,3} graphite-like layers in (b) is highlighted by the colouring; layers are coloured red and magenta.

We close with examples of (7,3) nets. This topology, like those above, is "incommensurate" with the symmetries of E^3, and is therefore difficult to realize from conventional Euclidean geometric approaches. First, consider in generality the vertex density of (3,7) on the (4,6) tiling. From equations (3-4), it is clear that the (3,7) has two 2 vertices per 4-ring of the (4,6) tiling respectively. We choose two possible configurations; (i) four (half) vertices, one on each edge of the 4-ring, and (ii) two vertices within the 4-ring. Both can be extended symmetrically; the former with *2233* orbifold symmetry (Figures 9a, 9b) and the latter with *2223* orbifold symmetry (Figure 9d). The *2233* pattern contains two distinct 3-fold and 2-fold sites, most readily seen in the coloured tiling of Figure 9a. In common with the previous examples, both *2233* and *2223* patterns contain significant geometric flexibility. Again, specific examples of both are possible with (5,5) superposed on the regular {6,4} tiling (Figures 9c, 9e).

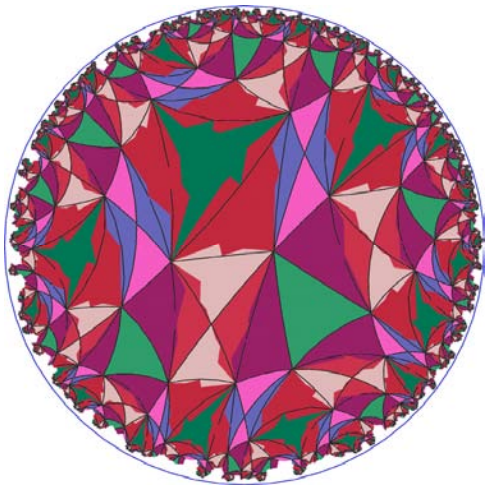

(a)

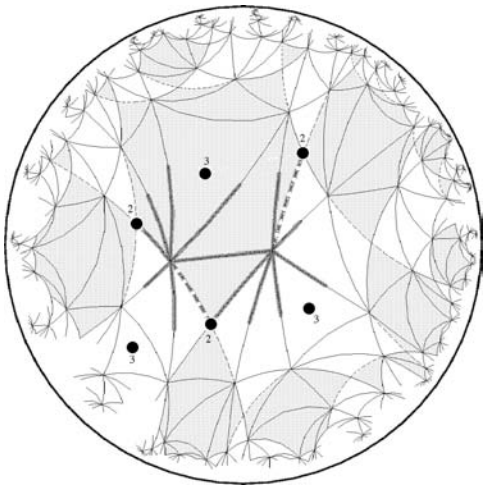

(b)

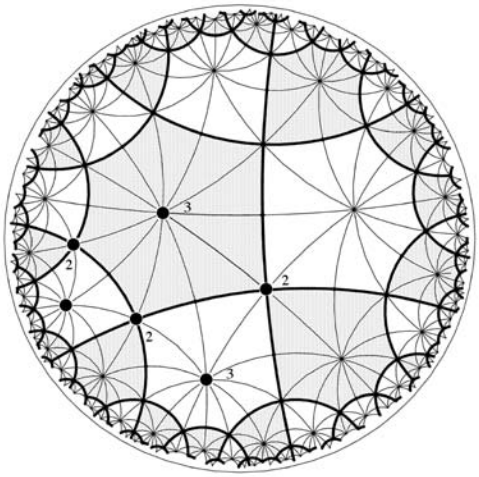

(c)

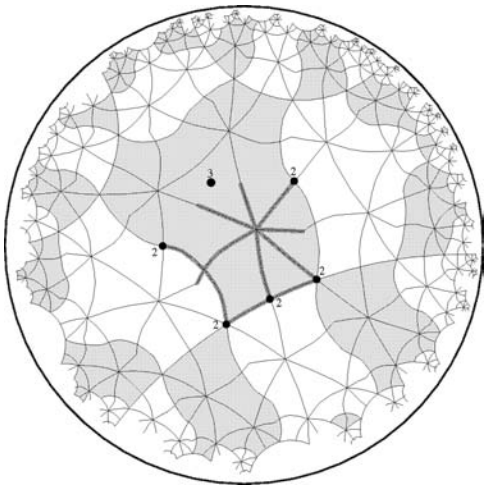

(d)

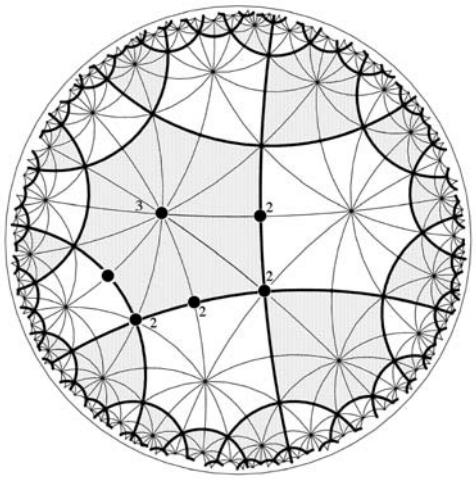

(e)

Figure 9: (a) Superpositions of an irregular (6,4) net on the (3,7) tiling. The resulting pattern has orbifold symmetry 2233. The pattern is coloured to reveal distinct 2-fold and 3-fold sites.
(b) The same tiling, with rotation centers within a single orbifold domain marked by dots (of orders 2 and 3). Full arcs belong to the (3,7) tiling; dotted arcs are appended to complete the (4,6) tiling. (Alternate (4) tiles are shaded for clarity.)
(c) The regular {6,4} tiling has a subgroup of symmetry 2233. (b) can therefore be deformed to give (7,3) on {6,4}.
(d)Superposition of (3,7) on (6,4) with 2223 symmetry. Rotation centers within a single orbifold domain are marked by dots. (Alternate (4) tiles are shaded for clarity.
(e) The regular {6,4} tiling has a subgroup of symmetry 2223. (d) can therefore be deformed to give (7,3) on {6,4}.

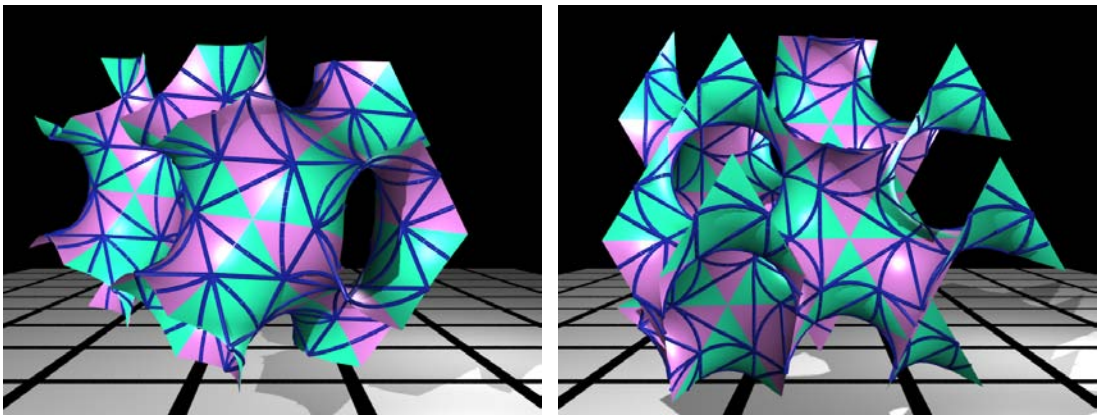

(a) (b)

Figure 10: (a,b) Projections of the 2233 pattern on the P and D surfaces respectively.

These patterns can be projected onto the P and D surfaces to give rather irregular (7,3) nets. The irregularity is particularly evident in the projected (7,3) patterns with *2223* symmetry, where extreme crowding of adjacent edges is evident on both the P and D projections (Figures 11a, 11c). Nevertheless, "relaxation" of the nets by relative vertex motion in E^3, to force a net with equal edge lengths and maximal E^3 symmetry[2] results in a very uniform net with cubic symmetry (space group $Fd\underline{3}$). (Detailed discussion of the relaxation and symmetrisation process in E^3 can be found elsewhere[13].) The edges are those of an array of regular icosahedra, interlinked in a diamond-like geometry by face-sharing with regular octahedra[2]. This embedding is conjectured to be the lowest density stable sphere packing[2].

The *2223* orbifold has characteristic $\frac{-1}{6}$ (index 4 and 14 relative to the **246* and **237* orbifolds respectively); the *2233* pattern has characteristic $-\frac{1}{3}$ (index 8 and 28 relative to the **246* and **237* orbifolds respectively). The ratio of characteristics of the regular (3,7) (**237)* and **246* orbifolds is equal to $\frac{84}{24}$, implying the possibility of a maximally

symmetric common sub-group of index 2 relative to **246* and 7 relative to **237*, with characteristic $\frac{-1}{12}$. Therefore, the possibility of a third, more symmetric (3,7) pattern on {4,6} cannot be ruled out *a priori*, though we have not been able to identify it.

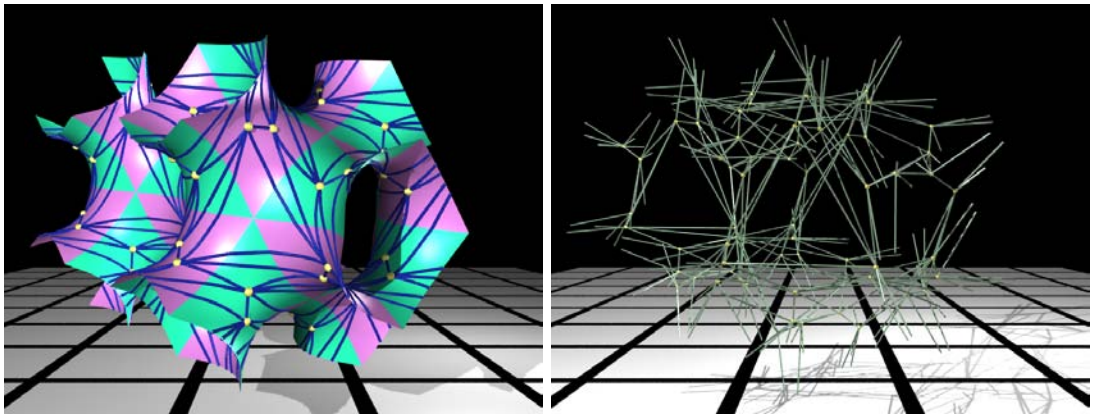

(a) (b)

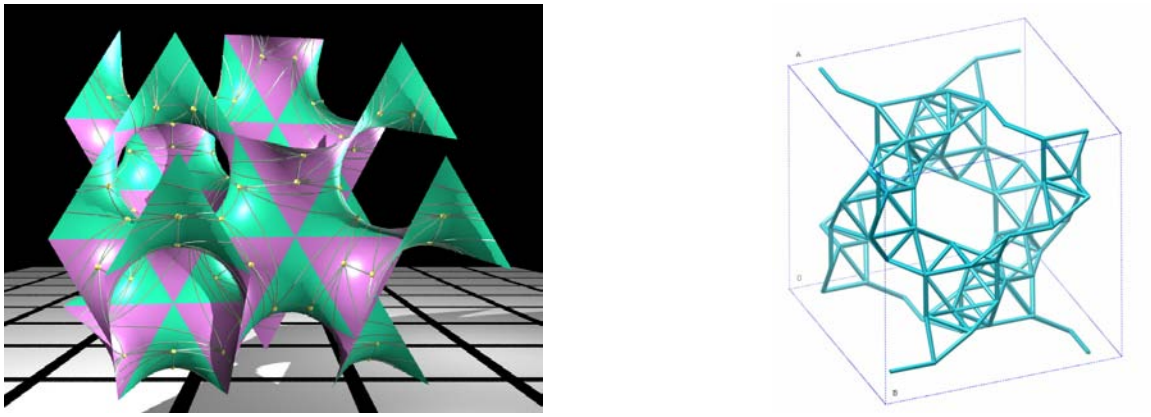

(c) (d)

Figure 11: (a), (c) Projections of the 2223 pattern onto the P and D surfaces respectively.
(b)Straightened version of (a), with fixed vertices (identical to those in (a)) and straight edges.
(d) Relaxed version of (g), a known very low density stable sphere packing (single unit cell displayed).

Conclusion:

Finally, we mention the possibility of mapping these hyperbolic patterns onto other three-periodic minimal surfaces. The procedure is not limited to the simpler three-periodic minimal surfaces. The atlas for the H surface, illustrated in Figures 2-3, allows construction of reticulations of that surface. Similarly, higher genus surfaces, such as the

I-WP surface can be handled. (Indeed, the orbifold defining the surface atlas of the I-WP surface – **2424* – is readily related to that of the P and D surfaces.)

We intend to automatically generate networks in E^3 with this technique. Given the richness of hyperbolic tilings, we expect some novel structures to emerge. The examples shown here demonstrate that possibility. The major challenge is likely to be the choice of an optimal "basis set" likely to lead to the most regular nets in E^3. We are faced with an embarrassing wealth of possibilities, both in numbers of hyperbolic tilings and variety of surfaces in E^3 to reticulate. The examples presented here are based on the P and D surfaces only. However, the variety of forms realised in those cases alone suggests that we can choose a small set of surfaces to reticulate without compromising the variety of resulting nets.

Appendix: Generation of hyperbolic patterns

The H^2 tilings have been generated using the public domain software *Funtiles* written by Daniel Huson[14]. The package relies on Delaney-Dress tiling symbols, described in detail elsewhere by Huson and colleagues[3,15,16,17]. The concept of these symbols is to encode the tiling pattern and symmetry by decomposition of the (2D) tiling into simplices, whose vertices lie on a face (*2*-vertex), edge (*1*-vertex) and vertex (*0*-vertex) of the original tiling. (The restriction to 2D is ours only: the approach is immediately generalisable to arbitrary dimensions.) Edges of the simplices are labeled by the index of the opposite vertex in that simplex (0,1 or 2). Simplices are labeled according to the symmetry of the pattern; symmetrically identical simplices carry identical labels. (Regular tilings have a single simplex only, the least symmetric (*n*,*z*) tilings have at most 2*n* simplices and 2*z* simplices per distinct face and edge respectively.) Involutions between adjacent simplexes are characterized by the label of the common simplex edge: e.g. a simplex of label *A* adjacent to one of label *B*, with common simplex edge *2* implies {*A*,*B*} lie within the class of *2*-involutions. The resulting encoding allows for an efficient tiling signature. A related concept has been suggested to us by John Conway; we call it here the Conway crankshaft (private communication). Let distinct simplices occupy distinct rows. Involutions between distinct simplices by *0*, *1* or *2*-edges are coded by edges linking those simplex entries in the *0*, *1* or *2* column. The columns contain *0-1* and *1-2* pairs, in order to collect face and vertex configurations of the original tiling respectively. The topology of each face and vertex connectivity is appended by adding the relevant digit to each component of the Conway crankshaft (face order, *n* and connectivity, *z*). The presence of symmetry elements can be discerned by inspection from the crankshaft topology, in common with the symmetry identification from Delaney-Dress symbols[16]. For example, mirror lines lead to (open) chains in the crankshaft diagram, while rotation centres lead to (closed) cycles. We list crankshaft diagrams for the H^2 tilings below. (The apparent reduced complexity of *0-1* and *1-2* cycles (faces and vertices respectively) is induced by the ordering of simplices we have chosen; shuffling of row orders is possible, provided the crankshat topology is unchanged.) These diagrams afford a concise signature of the tilings, and possible combinatorics of the crankshaft diagram consistent with the orders of *n* and *z* allow exhaustive listing of allowed tilings[16].

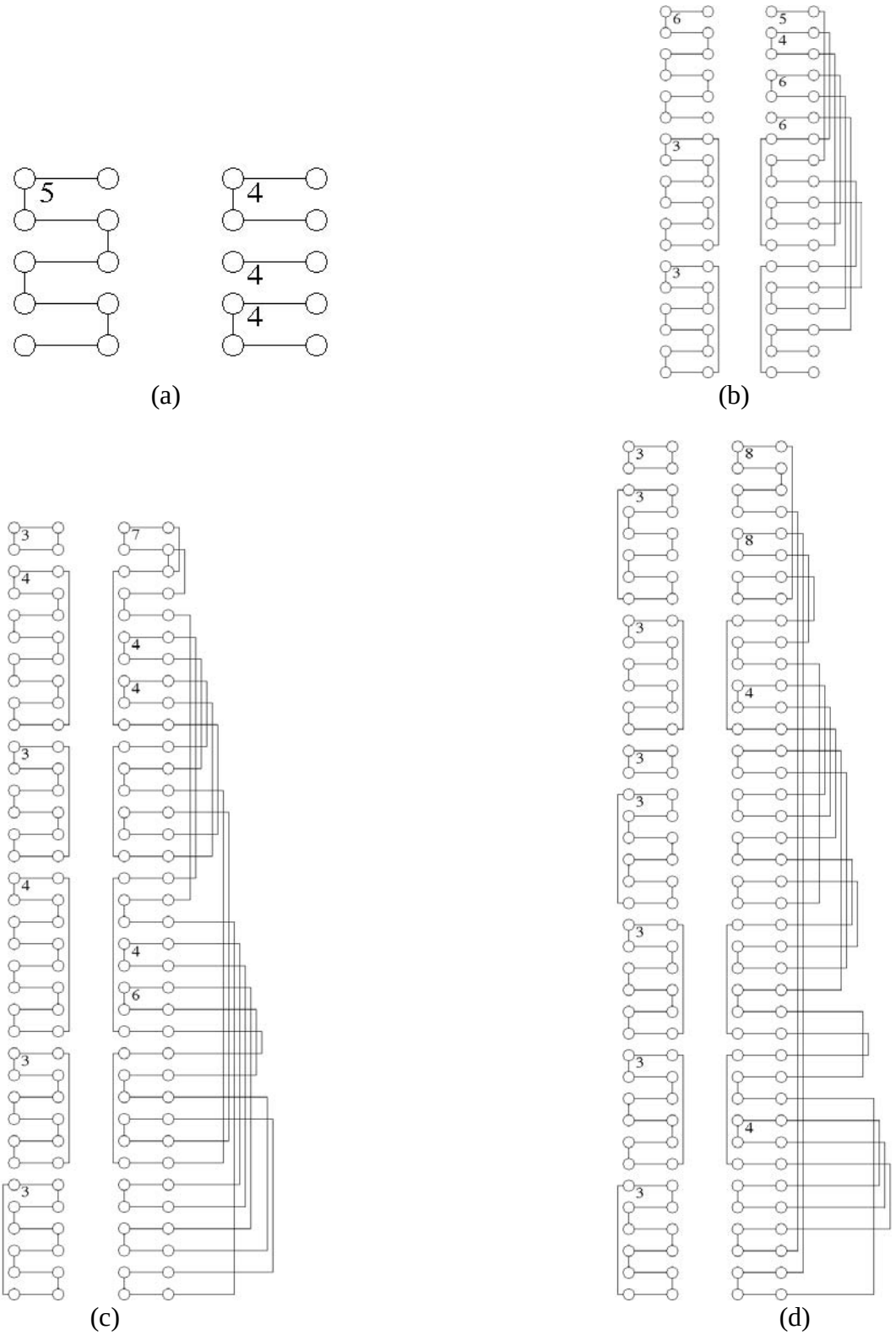

*Figure A1:Conway crankshaft diagrams for the (a) (5,4)+(6,4) tiling (symmetry *2224) shown in Figure 5a, (b) (5,5)+(6,4) tiling of Fig.7a (symmetry 22*2), (c) (3,7)+(6,4) tiling (symmetry 2233) of Figure 9b and (d) (3,7)+(6,4) tiling (symmetry 2323) in Fig.9d.*

References:

[1] Sadoc, J.F.; Mosseri, R. *Geometrical Frustration*; Cambridge University Press; Cambridge; 1999.
[2] O'Keeffe, M.; Hyde, B.G. *Crystal Structures 1. Patterns and Symmetry*; (Appendix 3) Mineralogical Society of America; Washington D.C.; 1996.
[3] Friedrichs, O.D.; Dress, A.W.M.; Huson, D.H.; Klinowski J.; Mackay, A.L.; *Nature*, **1999**, *400*, 644.
[4] Andersson, S; *Angew. Chem.*, **1983**, *22*, 69.
[5] Mackay, A.L.; *Proc. Roy. Soc. Lond. A*, **1993**, *442*, 47.
[6] Stillwell, J.; *Geometry of Surfaces*, Springer-Verlag; N.Y.;1992.
[7] Fogden, A.; Hyde, S.T.; *Acta Crystallogr A*, **1992**, *48*, 442-451, 575-591.
[8] Hyde, S.T.; Oguey, C.; *Eur. Phys. J. B*, **2000**, *16*, 613.
[9] Sadoc, J.-F; Charvolin, J; *Acta Cryst A* **1989**, *45*, 10.
[10] Conway, J.H In *Groups, Combinatorics and Geometry* London Mathematical Society Lecture Notes; Cambridge University Press; Cambridge; 1992.
[11] Hilbert, D.; Cohn-Vossen, S; *Geometry and the Imagination*; Chelsea Publishing Company; N.Y.; 1952.
[12] Hyde S.T; Ramsden, S. IN *Chemical Topology. Applications and Techniques;* Mathematical Chemistry Series, volume 6; Bonchev, D; Rouvray D.H., Eds, Gordon and Breach Science Publishers; Amsterdam, 2000.
[13] Hyde, S.T; Ramsden, S; Di Matteo, T; Longdell, J; *Solid State Sciences*, in press (2002).
[14] <www.mathematik.uni-bielefeld.de/~huson/papers.html>
[15] Huson, D.H.; *Geometriae Dedicata* **1993**, *47*, 269.
[16] Balke, L.; Huson, D.H.; *Geometriae Dedicata* **1996**, *60*, 89.
[17] Delgado Friedrichs, O; < www.mathematik.uni-bielefeld.de/~delgado/TCS/text.html>.